Supplementary Material: Accelerating Robotic Reinforcement Learning via Parameterized Action Primitives

Anonymous Author(s)
Affiliation
Address
`email`

Submitted to 35th Conference on Neural Information Processing Systems (NeurIPS 2021). Do not distribute.

A Results and Visualizations

Website with Video Results: Video results are provided in the supplementary zip file. To make it easier to review the result videos, we have also hosted them at the following anonymized website: https://sites.google.com/view/neurips2021raps.

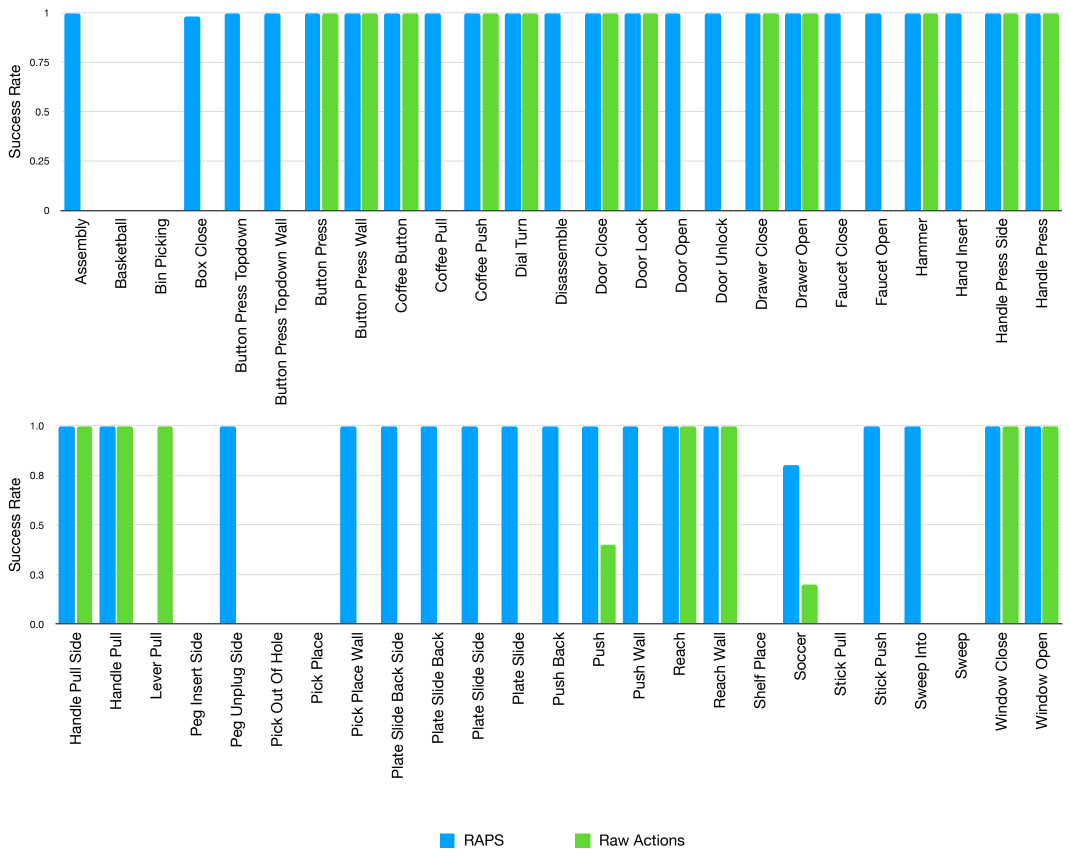

Figure 1: Final performance results for single task RL on the Metaworld domain after 3 days of training using the Dreamer base algorithm. RAPS is able to successfully learn most tasks, solving 43 out of 50 tasks while Raw Actions is only able to solve 21 tasks. See full results plots in Figure 7.

Cross Robot Transfer We train a higher level policy over RAPS from visual input to solve the door opening task in Robosuite using the xARM 7. We then directly transfer this policy (zero-shot) to an xARM 6 robot. The transferred policy is able to achieve **100%** success rate on the door opening task with the 6DOF robot while trained on a 7DOF robot. This is possible due to the robot agnostic property of RAPS.

Comparison against Dynamic Motion Primitive Methods As noted in the related works section, Dynamic Motion Primitives (DMP) are an alternative skill formulation that is common robotics literature. We compared RAPS with the latest state-of-the-art work that incorporates DMPs with deep RL: Neural Dynamic Policies [1]. As seen in Figure 5, across nearly every task in the Kitchen suite, RAPS outperforms NDP just as it outperforms all prior skill learning methods as well.

B Environments

We provide detailed descriptions of each environment suite and the specific tasks each suite contains. All environments use the MuJoCo simulator [7].

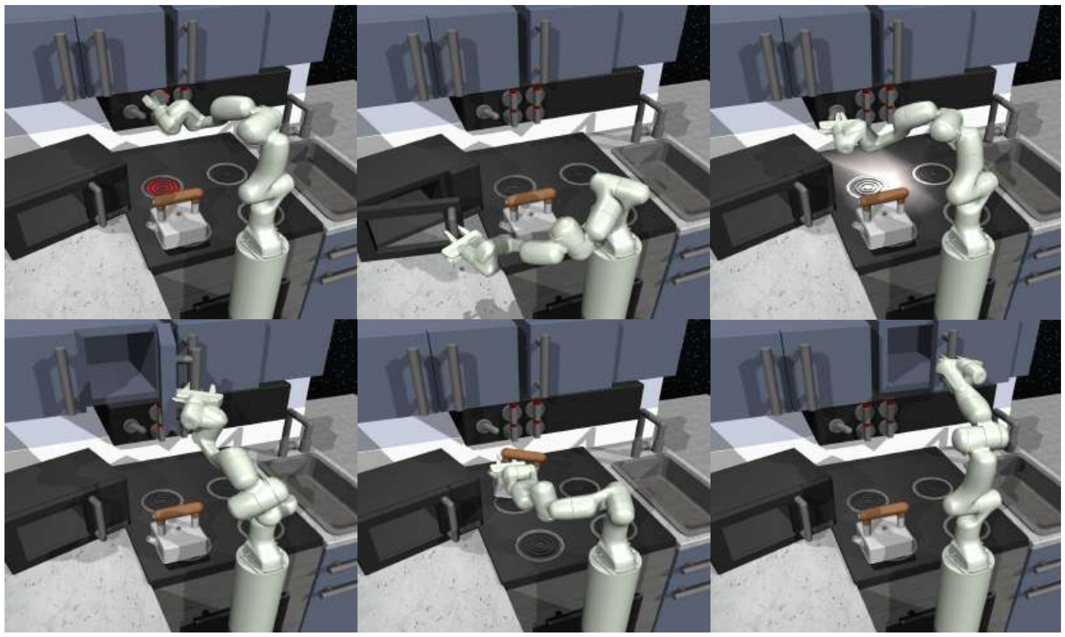

Figure 2: Visual depiction of the Kitchen environment; all tasks are contained within the same setup. Each image depicts the solution of one of the tasks, we omit the bottom burner task as it is the goal is the same as the top burner task, just with a different dial to turn. For the top row from the left: `top-left-burner`, `microwave`, `light-switch`. For the bottom row from the left: `hinge-cabinet`, `kettle`, `slide cabinet`.

B.1 Kitchen

The Kitchen suite, introduced in [2], involves a set of different tasks in a kitchen setup with a single Franka Panda arm as visualized in Figure 2. This domain contains 7 subtasks: `slide-cabinet` (shift right-side cabinet to the right), `microwave` (open the microwave door), `kettle` (place the kettle on the back burner), `hinge-cabinet` (open the hinge cabinet), `top-left-burner` (rotate the top stove dial), `bottom-left-burner` (rotate the bottom stove dial), and `light-switch` (flick the light switch to the left). The tasks are all defined in terms of a sparse reward, in which $+1$ reward is received when the norm of the joint position (qpos in MuJoCo) of the object is within .3 of the desired goal location and 0 otherwise. See the appendix of the RPL [2] paper for the exact definition of the sparse and the dense reward functions in the kitchen environment. Since the rewards are defined simply in terms of distance of object to goal, the agent does not have to execute interpretable behavior in order to solve the task. For example, to solve the burner task, it is possible to push it to the right setting without grasping and turning it.

For the sequential multi-task version of the environment, in a single episode, the goal is to complete four different subtasks. The agent receives reward once per sub-task completed with a maximum episode return (sum of rewards) of 4. In our case, we split the 7 tasks in the environment into two multi-task environments which are roughly split on difficulty. We define the two multi-task environments in the kitchen setup: `Kitchen Multitask 1` which contains `microwave`, `kettle`, `light-switch` and `top-left-burner` while `Kitchen Multitask 2` contains the `hinge-cabinet`, `slide-cabinet`, `bottom-left-burner` and `light-switch`. As mentioned in the experiments section, RL trained on joint velocity control is unable to solve almost any of the single task environments using image input from sparse rewards. Instead, we modify the environment to use 6DOF delta position control by adding a mocap constraint as implemented in Metaworld [8].

B.2 Metaworld

Metaworld [8] consists of 50 different manipulation environments in which a simulated Sawyer Rethink robot is charged with solving tasks such as faucet opening/closing, pick and place, assem-

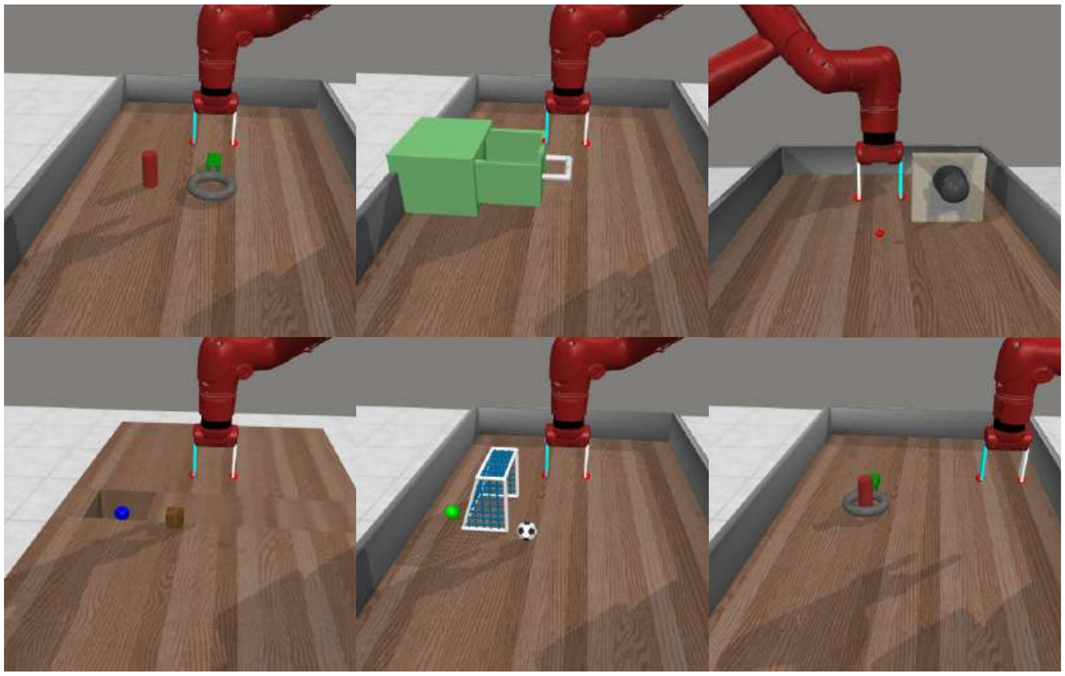

Figure 3: Visual depiction of the Metaworld environment suite. For the top row from the left: `assembly-v2`, `drawer-close-v2`, `peg-unplug-side-v2`. For the bottom row from the left: `sweep-into-v2`, `soccer-v2`, `disassemble-v2`.

bly/disassembly and many others. Due to computational considerations, we selected 6 tasks which range from easy to difficult: `drawer-close-v2` (push the drawer closed), `hand-insert-v2` (place the hand inside the hole), `soccer-v2` (hit the soccer ball to a specific location in the goal box), `sweep-into-v2` (push the block into the hole), `assembly-v2` (grasp the nut and place over the thin block), and `disassembly-v2` (grasp the nut and remove from the thin block).

In Metaworld, the raw actions are delta positions, while the end-effector orientation remains fixed. For fairness, we disabled the use of any rotation primitives for this suite. Metaworld has a hand designed dense reward per task which enables efficient learning, but is unrealistic for the real world in which it can be challenging to design dense rewards without access to the true state of the world. Instead, for more realistic evaluation, we run all methods with a sparse reward which uses the success metric emitted by the environment itself.

We run the environments in single task mode, meaning the target positions remain the same across experiments, in order to evaluate the basic effectiveness of RL across action spaces. This functionality is provided in the latest release of Metaworld. Additionally, we use the V2 versions of the tasks after correspondence with the current maintainers of the benchmark. The V2 environments have a more realistic visual appearance, improved reward functions and are now the primarily supported environments in Metaworld. See Figure 3 for a visualization of the Metaworld tasks.

B.3 Robosuite

Robosuite is a benchmark of robotic manipulation tasks which emphasizes realistic simulation and control while containing several tasks existing RL algorithms struggle to solve, even when provided state based information and dense rewards. This suite contains a torque based end-effector position control implementation, Operational Space Control [4]. We select the `lift` and `door` tasks for evaluation, which we visualize in Figure 4. The lifting task involves accurately grasping a small red block and lifting it to a set height. The door task involves grasping the door handle, pushing it down to unlock it and pulling it open to a set position. These tasks contain initial state randomization; at each reset the position of the block or door is randomized within a small range. This property makes the Robosuite tasks more challenging than Kitchen and Metaworld, both of which are deterministic environments. For this environment, sparse rewards were already defined so we directly use them in

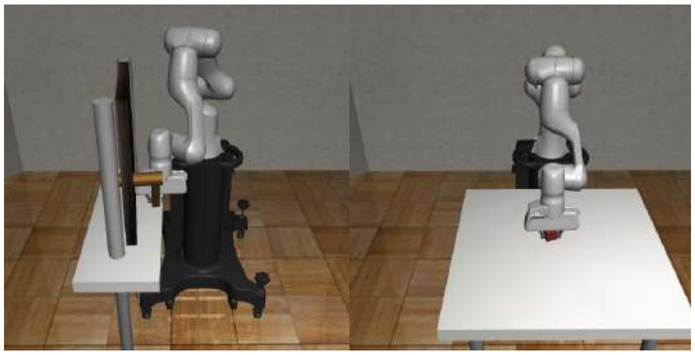

Figure 4: Visual depiction of the Robosuite environments. On the left we have the door opening task, and on the right we have the block lifting task.

our experiments. We made several changes to these environments to improve learning performance of the baselines as well as RAPS. Specifically, we included a workspace limit in a large area around the object, which improves exploration in the case of sparse rewards. For the lifting task, we increased the frequency of the default OSC controller to 40Hz from 20Hz, while for the door opening task we changed the max action magnitude to .1 from .05.

C Primitive Implementation Details

In this section, we provide specific implementation details regarding the primitives we use in our experiments. In particular, we use an end-effector pose controller as C_k for all k. We compute the target state s^* using the components of the robot state which correspond to the input arguments of the primitive, s_{args}. We compute s^* using the formula $s^* = s_{\text{args}} + \text{args}$. The error metric is computed in a similar manner $e_k = s^* - s_{\text{args}}$ across primitives. Returning to the lifting primitive example in the main text, s_{args} would be the z position of the end-effector, s^* would be the target z position after lifting, and e_k would be the difference between the target z position and the current z position of the end-effector. In Table 4 we provide additional details regarding each primitive including the search spaces, number of low-level actions and which environment it was used in. One primitive of note is go to pose (delta) which performs delta position control. Using this primitive alongside the grasp and release primitives corresponds closely to the raw action space for Metaworld and Robosuite, environment suites in which we do not use orientation control.

We tuned the low-level actions per environment suite, but one could alternatively design a tolerance threshold and loop until it is achieved to avoid any tuning. We chose a fixed horizon which runs significantly faster and any inaccuracies in the primitives are accounted for by the learned policy. Finally, we do not use every primitive in every domain, yet across all tasks within a domain we use the same library. In Metaworld, the raw action space does not allow for orientation control so we do not either. Enabling orientation control with primitives can, in certain cases, make the task easier, but we do not include the x-axis and y-axis rotation primitives for fair comparison. In Robosuite, the default action space has orientation control. We found orientation control was unnecessary in order to solve the lifting and door opening tasks when we disabled orientation control for raw actions and for primitives. As a result, in this work we report results without orientation control in Robosuite.

D RL Implementation Details

Whenever possible, we use the original implementations of any method we compare against. We use standard implementations for each base RL algorithm except Dreamer, which we implement in PyTorch. We use the actor and model hyper-parameters from Dreamer-V2 [3] as we found it slightly improved the performance of Dreamer. For primitives, we made several hyper-parameter changes to better tailor Dreamer to hybrid discrete-continuous control. Specifically, instead of backpropagating the return through the dynamics, we use REINFORCE to train the actor in imagination. We additionally reduce the imagination trajectory length from 15 to 5 for the single task primitive experiments since the trajectory length is limited to 5 in any case. With the short trajectory lengths in RAPS,

Hyper Parameter	Value
Actor output distribution	Truncated Normal
Discount factor	0.99
λ_{GAE}	0.95
actor and value function learning rates	8e-5
world model learning rate	3e-4
Imagination horizon	15
Entropy coefficient	1e-4
Predict discount	No
Target value function update period	100
reward loss scale	2
Model hidden size	400
Stochastic state size	50
Deterministic state size	200
Embedding size	1024
RSSM hidden size	200
Use GRU layer norm	Yes
Actor hidden layers	4
Value hidden layers	3
batch size	50
batch length	50

Table 1: Dreamer hyper-parameters

imagination often goes beyond the end of the episode, so we use a discount predictor to downweight imagined states beyond the end of the episode. Finally since we cannot sample batch lengths of 50 from trajectories of length 5 or 15, we instead sample the full primitive trajectory and change the batch size to be $\frac{2500}{H}$, the primitive horizon. This results in an effective batch size of 2500, which is equal to the Dreamer batch size of 50 with a batch length of 50.

In the case of SAC, we use the implementation of SAC [6] but without data augmentation, which amounts to using their specific pixel encoder which we found to perform well. Finally for PPO, we use the following implementation: Kostrikov [5]. See Tables 1, 2, 3 for the hyper-parameters used for each algorithm respectively. We use the same algorithm hyper-parameters across all the baselines. For primitives, we modify the discount factor in all experiments to $1 - \frac{1}{H}$, in which H is the primitive horizon. This encourages the agent to highly value near term rewards with short horizons. For single task experiments, we use a horizon of 5, taking 5 primitive actions in one episode, with a discount of 0.8. For the hierarchical control experiments we use a horizon of 15 and a corresponding discount of $.93$. In practice, this method of computing the discount factor improves the performance and stability of RAPS.

For each baseline we use the original implementation when possible as an underlying action space for each RL algorithm. For VICES, we take the impedance controller from the iros_19_vices branch and modify the environment action space to output the parameters for the controller. For PARROT, we use an unreleased version of the code provided by the original authors. For SPIRL, we use an improved version of the method which was released to the SPIRL code base recently. This version, SPIRL-CL, uses a closed loop decoder to map latents back to action trajectories which they find significantly improves performance on the Kitchen environment from state input. We use the authors' code for vision-based SPIRL-CL and still find that RAPS performs better.

Hyper Parameter	Value
Discount factor	0.99
actor, critic, encoder learning rates	2e-4
alpha learning rate	1e-4
Target network update frequency	2
Polyak averaging constant	.01
Frame stack	4
Image size	64
Random policy warm up steps	2500
batch size	512

Table 2: SAC hyper-parameters

Hyper Parameter	Value
Entropy coefficient	.01
Value loss coefficient	0.5
Actor-value network learning rate	3e-4
Number of mini-batches per epoch	10
PPO clip parameter	0.2
Max gradient norm	0.5
λ_{GAE}	0.95
Discount factor	0.99
Number of parallel environments	12
Frame stack	4
Image size	84

Table 3: PPO hyper-parameters

Primitive Skill	**Parameters**	**Action Space**	**# low-level actions**	**Environments**
grasp	d	[0,1]	150-200	Kitchen, Metaworld, Robosuite
release	d	[-1,0]	200-300	Kitchen, Metaworld, Robosuite
lift	z	[0, 1]	40-300	Kitchen, Metaworld, Robosuite
drop	z	[-1, 0]	40-300	Kitchen, Metaworld, Robosuite
push	y	[0, 1]	40-300	Kitchen, Metaworld, Robosuite
pull	y	[-1, 0]	40-300	Kitchen, Metaworld, Robosuite
shift right	x	[0, 1]	40-300	Kitchen, Metaworld, Robosuite
shift left	x	[-1, 0]	40-300	Kitchen, Metaworld, Robosuite
go to pose (delta)	x,y,z	$[-1, 0]^3$	40-300	Kitchen, Metaworld, Robosuite
x-axis twist	θ	$[-\pi, \pi]$	300	Kitchen
y-axis twist	θ	$[-\pi, \pi]$	300	Kitchen
angled forward grasp	θ, x, y, d	$[-\pi, \pi]$, $[-1, 0]^3$	1100	Kitchen
top z grasp	z,d	$[-1, 0]^2$	140-250	Robosuite
top grasp	x,y,z,d	$[-1, 0]^4$	1500	Metaworld

Table 4: Description of skill parameters, search spaces, low-level actions and environment usage.

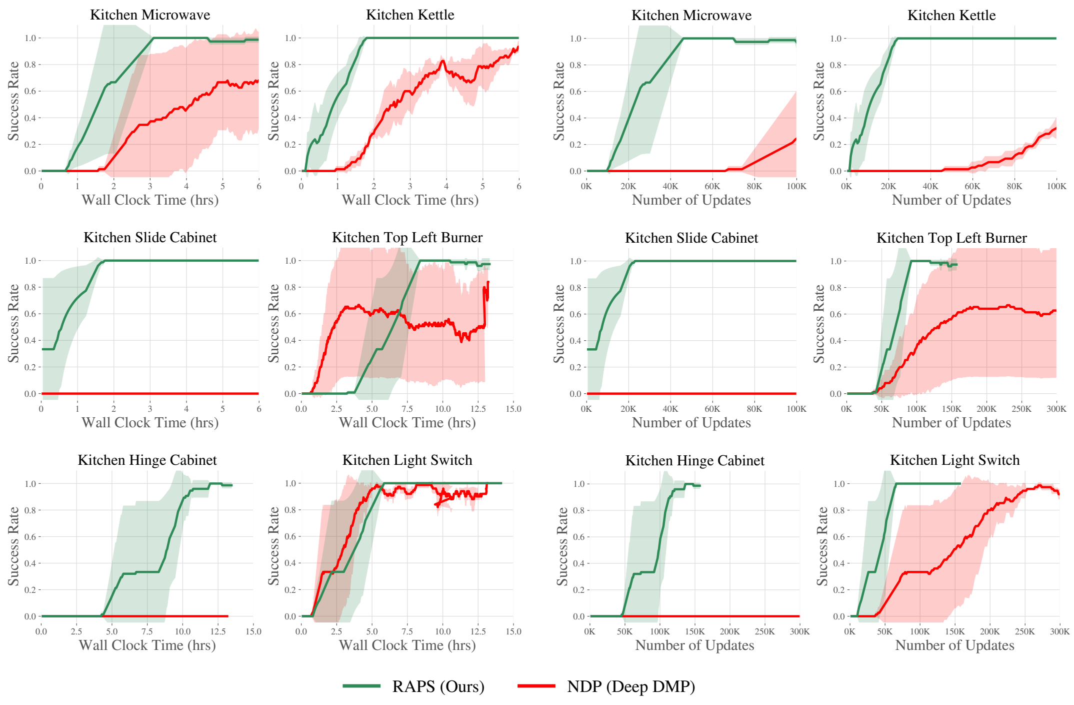

Figure 5: Comparison of RAPS against NDP, a deep DMP method for RL. RAPS dramatically outperforms NDP on nearly every task from visual input, both in terms of wall-clock time and number of training steps. This result demonstrates the increased capability of RAPS over DMP-based methods.

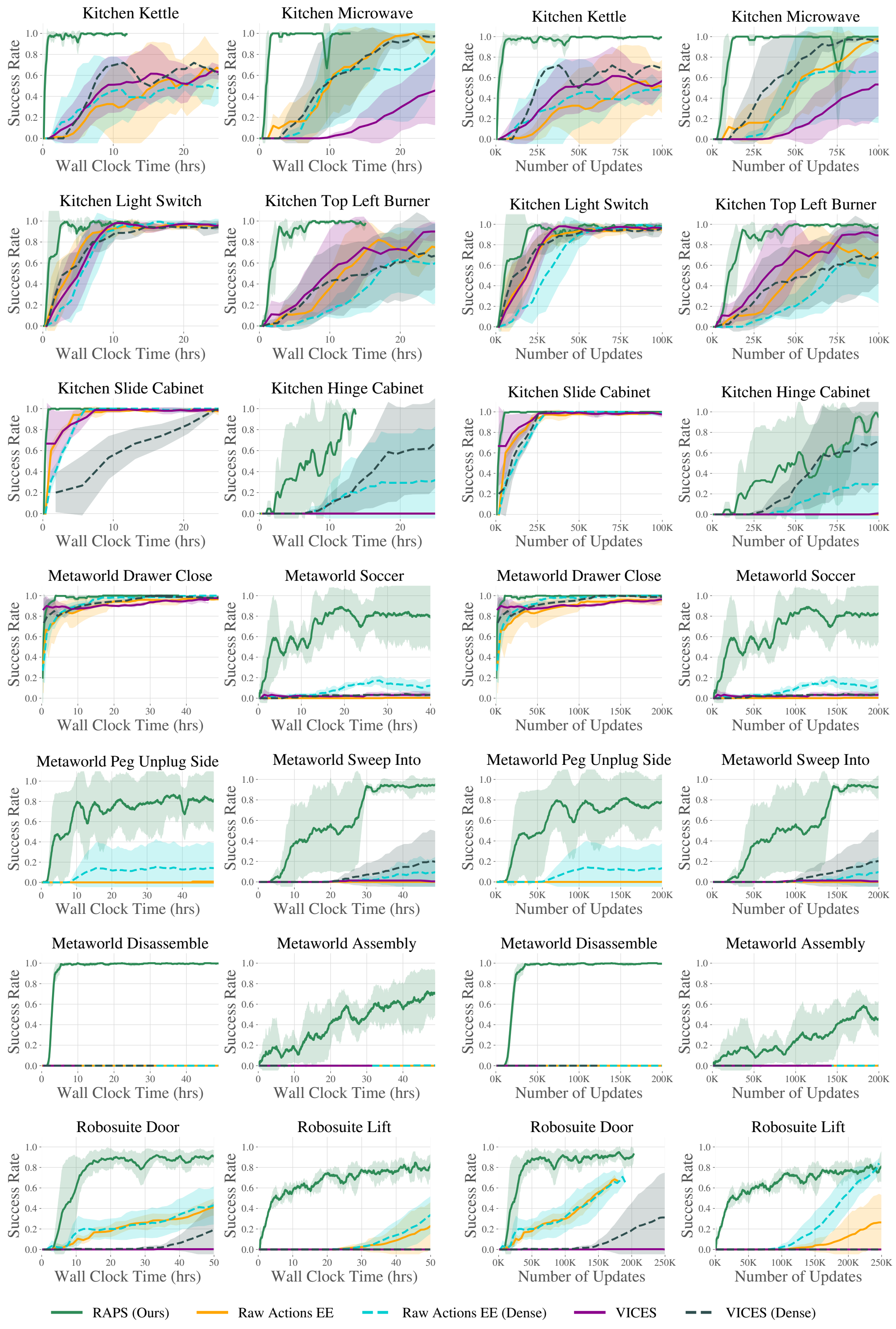

Figure 6: Full version of Figure 3 with excluded environments (`slide-cabinet` and `soccer-v2`) and plots against number of updates (right two columns). RAPS outperforms all baselines against number of updates as well.

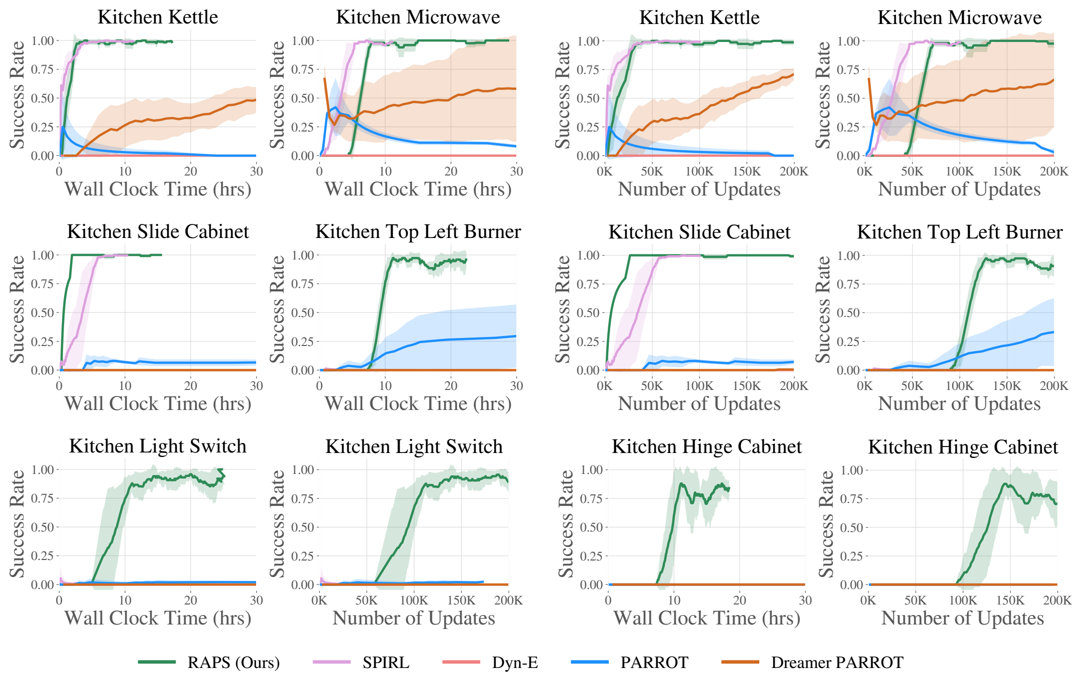

Figure 7: Full version of Figure 4 with plots against number of updates (right column) and excluded environments (`light-switch`). While SPIRL is competitive with RAPS on the easier tasks, it fails to make progress on the more challenging tasks.

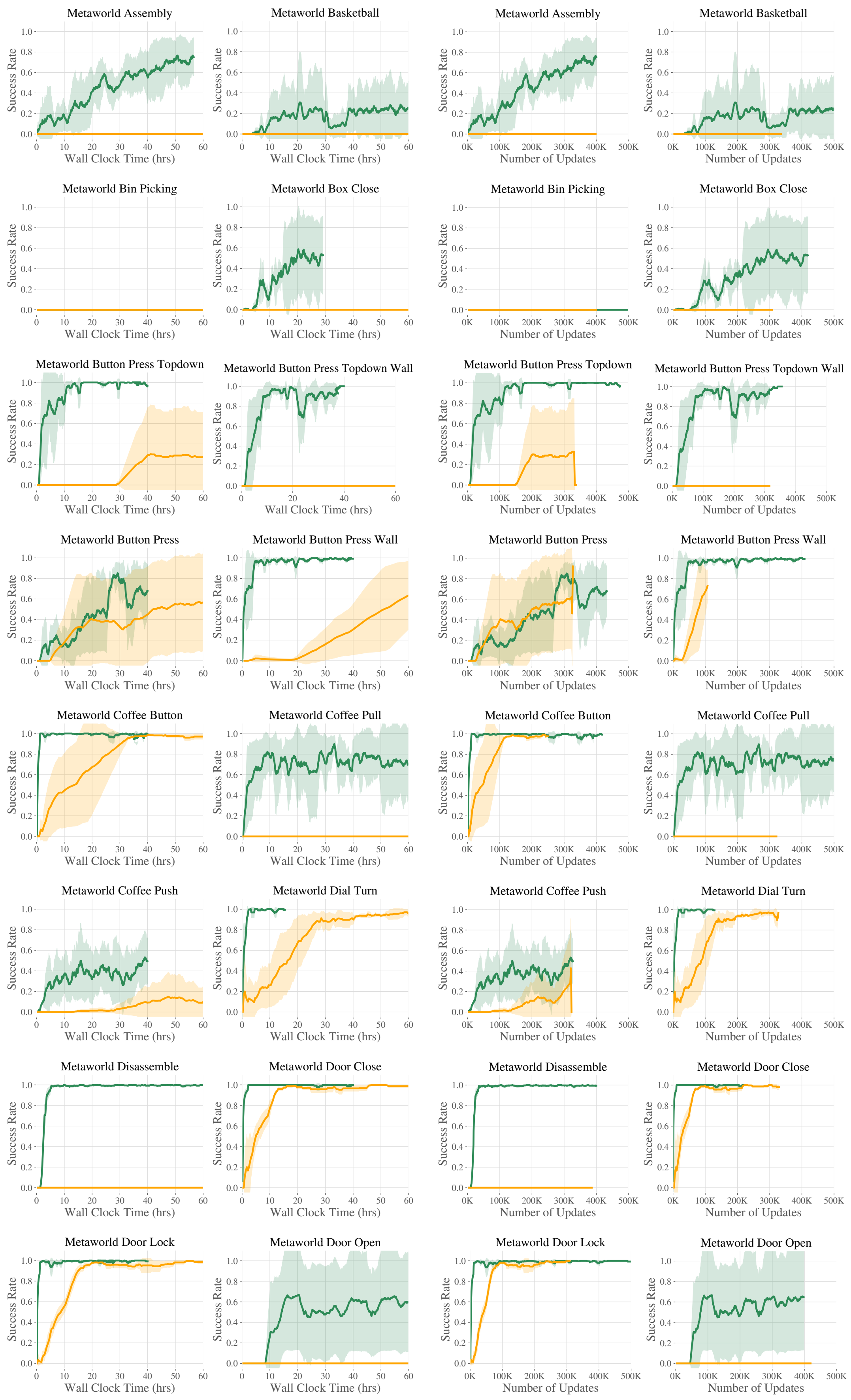
Metaworld Assembly
Metaworld Basketball
Metaworld Assembly
Metaworld Basketball
Metaworld Bin Picking
Metaworld Box Close
Metaworld Bin Picking
Metaworld Box Close
Metaworld Button Press Topdown
Metaworld Button Press Topdown Wall
Metaworld Button Press Topdown
Metaworld Button Press Topdown Wall
Metaworld Button Press
Metaworld Button Press Wall
Metaworld Button Press
Metaworld Button Press Wall
Metaworld Coffee Button
Metaworld Coffee Pull
Metaworld Coffee Button
Metaworld Coffee Pull
Metaworld Coffee Push
Metaworld Dial Turn
Metaworld Coffee Push
Metaworld Dial Turn
Metaworld Disassemble
Metaworld Door Close
Metaworld Disassemble
Metaworld Door Close
Metaworld Door Lock
Metaworld Door Open
Metaworld Door Lock
Metaworld Door Open
Success Rate
Wall Clock Time (hrs)
Number of Updates

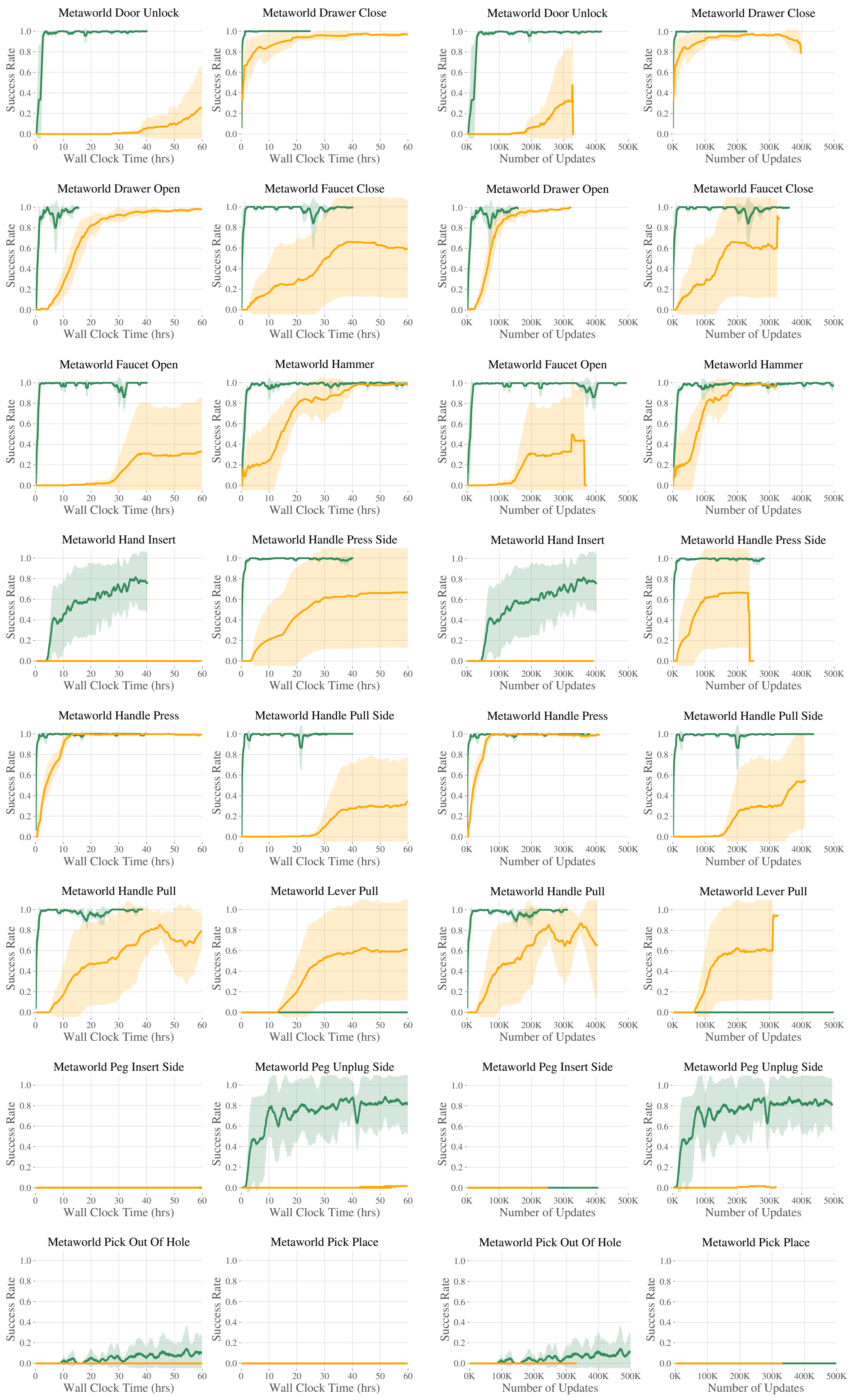
Metaworld Door Unlock
Metaworld Drawer Close
Metaworld Door Unlock
Metaworld Drawer Close
Metaworld Drawer Open
Metaworld Faucet Close
Metaworld Drawer Open
Metaworld Faucet Close
Metaworld Faucet Open
Metaworld Hammer
Metaworld Faucet Open
Metaworld Hammer
Metaworld Hand Insert
Metaworld Handle Press Side
Metaworld Hand Insert
Metaworld Handle Press Side
Metaworld Handle Press
Metaworld Handle Pull Side
Metaworld Handle Press
Metaworld Handle Pull Side
Metaworld Handle Pull
Metaworld Lever Pull
Metaworld Handle Pull
Metaworld Lever Pull
Metaworld Peg Insert Side
Metaworld Peg Unplug Side
Metaworld Peg Insert Side
Metaworld Peg Unplug Side
Metaworld Pick Out Of Hole
Metaworld Pick Place
Metaworld Pick Out Of Hole
Metaworld Pick Place
Success Rate
Wall Clock Time (hrs)
Number of Updates
0.0
0.2
0.4
0.6
0.8
1.0
0
10
20
30
40
50
60
0K
100K
200K
300K
400K
500K

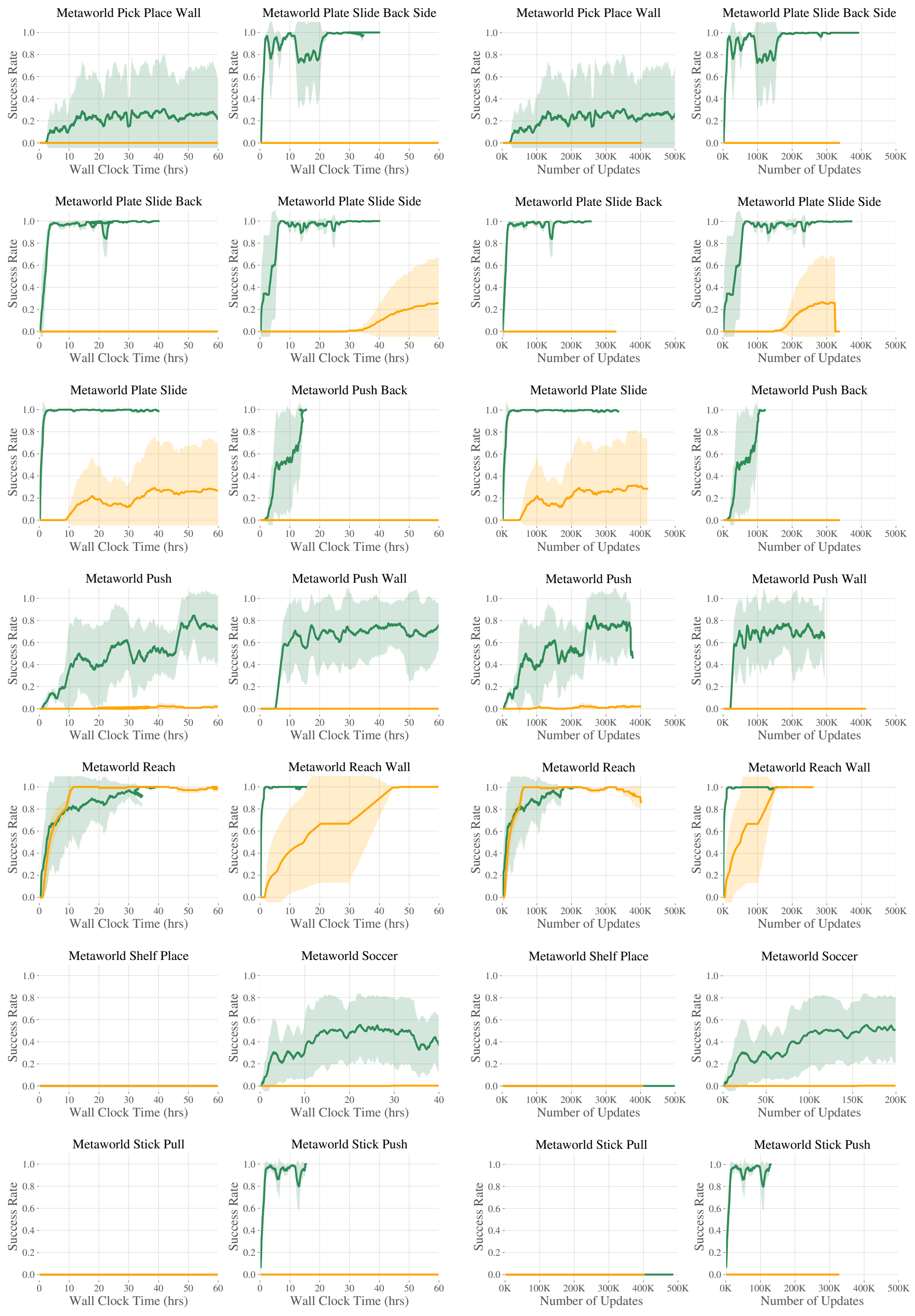

Metaworld Pick Place Wall
Metaworld Plate Slide Back Side
Metaworld Pick Place Wall
Metaworld Plate Slide Back Side
Metaworld Plate Slide Back
Metaworld Plate Slide Side
Metaworld Plate Slide Back
Metaworld Plate Slide Side
Metaworld Plate Slide
Metaworld Push Back
Metaworld Plate Slide
Metaworld Push Back
Metaworld Push
Metaworld Push Wall
Metaworld Push
Metaworld Push Wall
Metaworld Reach
Metaworld Reach Wall
Metaworld Reach
Metaworld Reach Wall
Metaworld Shelf Place
Metaworld Soccer
Metaworld Shelf Place
Metaworld Soccer
Metaworld Stick Pull
Metaworld Stick Push
Metaworld Stick Pull
Metaworld Stick Push
Success Rate
Wall Clock Time (hrs)
Number of Updates

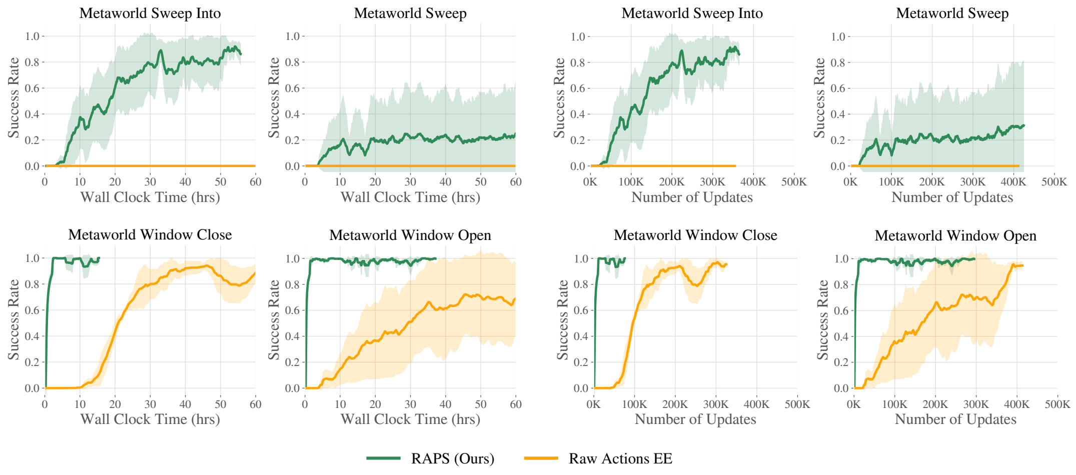

Figure 7: Comparison of RAPS against raw actions across all 50 Metaworld tasks from sparse rewards. RAPS is able to outright solve or make progress on up to **43 tasks** while Raw Actions struggles to make progress on most environments.

References

[1] S. Bahl, M. Mukadam, A. Gupta, and D. Pathak. Neural dynamic policies for end-to-end sensorimotor learning, 2020. 2

[2] A. Gupta, V. Kumar, C. Lynch, S. Levine, and K. Hausman. Relay policy learning: Solving long-horizon tasks via imitation and reinforcement learning, 2019. 3

[3] D. Hafner, T. Lillicrap, M. Norouzi, and J. Ba. Mastering atari with discrete world models. *arXiv preprint arXiv:2010.02193*, 2020. 5

[4] O. Khatib. A unified approach for motion and force control of robot manipulators: The operational space formulation. *IEEE Journal on Robotics and Automation*, 3(1):43–53, 1987. 4

[5] I. Kostrikov. Pytorch implementations of reinforcement learning algorithms. `https://github.com/ikostrikov/pytorch-a2c-ppo-acktr-gail`, 2018. 6

[6] M. Laskin, K. Lee, A. Stooke, L. Pinto, P. Abbeel, and A. Srinivas. Reinforcement learning with augmented data, 2020. 6

[7] E. Todorov, T. Erez, and Y. Tassa. MuJoCo: A physics engine for model-based control. In *The IEEE/RSJ International Conference on Intelligent Robots and Systems*, 2012. 2

[8] T. Yu, D. Quillen, Z. He, R. Julian, K. Hausman, C. Finn, and S. Levine. Meta-world: A benchmark and evaluation for multi-task and meta reinforcement learning. In *Conference on Robot Learning*, pages 1094–1100. PMLR, 2020. 3